[8] Spreeman, K. P., "Wind-Tunnel Investigation of Longitudinal Aerodynamic Characteristics of a Powered Four-Duct-Propeller VTOL Model in Transition," TN D-3192, April 1966, NASA.

[9] Newsom, W. A., Jr. and Freeman, D. C., Jr., "Flight Investigation of Stability and Control Characteristics of a 0.18-Scale Model of a Four-Duct Tandem V/STOL Transport," TN D-3055, April 1966, NASA.

[10] Tosti, L. P., "Longitudinal Stability and Control of a Tilt-Wing VTOL Aircraft Model With Rigid and Flapping Propeller Blades," TN D-1365, July 1962, NASA.

[11] Pegg, R. J., "Summary of Flight-Test Results of the VZ-2 Tilt-Wing Aircraft," TN D-989, Feb. 1962, NASA.

[12] Curtiss, H. C., Jr. and Putman, W. F., "Results of Experimental Correlation of Model and Full Scale Helicopter and VTOL Longitudinal Dynamics," Rept. 543, April 1961, Dept. of Aerospace and Mechanical Sciences, Princeton Univ., Princeton, N. J.

[13] Goldberg, J., "Stability and Control of Tandem Helicopters," Rept. 362, Sept. 1956, Dept. of Aerospace and Mechanical Sciences, Princeton Univ., Princeton, N. J.

[14] Schultz, E. R., "The Determination of Helicopter Longitudinal Stability Derivatives From Flight Test Data," WADC Technical Report 55-438, Pt. II, March 1959, Wright Air Development Center, Wright-Patterson Air Force Base, Ohio.

[15] Halley, D. H., "The Development of a Simplified Analytical Approach for Evaluation of the Dynamic Stability Characteristics of a Ducted-Propeller VTOL Aircraft in Transition," Rept. 850, Aug. 1968, Dept. of Aerospace and Mechanical Sciences, Princeton Univ., Princeton, N. J.

[16] Beppu, G. and Curtiss, H. C., Jr., "An Analytical Study of Factors Influencing the Longitudinal Stability of Tilt-Wing VTOL Aircraft," USAAVLABS Technical Report 66-53, July 1966, U. S. Army Aviation Materiel Labs., Fort Eustis, Va.

[17] Kirby, R. H., "Aerodynamic Characteristics of Propeller-Driven VTOL Aircraft," presented at NASA Conference on V/STOL Aircraft, Nov. 17–18, 1960, Langley Research Center, Langley Field, Va.

JAN.-FEB. 1970 J. AIRCRAFT VOL. 7, NO. 1

Fluctuating Flowfield of Propellers in Cruise and Static Operation

J. C. ERICKSON JR.*
Cornell Aeronautical Laboratory Inc., Buffalo, N. Y.

AND

GARY R. HOUGH†
University of Michigan, Ann Arbor, Mich.

The flowfields computed in the lifting-line approximation for finite-bladed, lightly loaded propellers in axial cruise are compared for constant and distributed blade circulations of the same total loading. Regions of agreement and differences in the two flowfields are distinguished for various blade numbers and advance ratios, and the asymptotic behavior of the velocity components is established. Related computations and comparisons are made for heavily loaded propellers in static operation, i.e., hover. A propeller in static operation is characterized by a greatly distorted trailing vortex system and the appreciable radial contraction and axial extension involved are modeled in the present numerical computations. The azimuthal variations of the velocity components in the propeller plane are presented for three cases which allow the velocity variations to be examined for three- and four-bladed propellers with similar effective pitch of their trailing vortex systems, and for two three-bladed propellers with widely different effective pitch. The relationship between the mean inflow at a given radius in the propeller disk plane and the instantaneous inflow to the blades at the same radius is examined for these same three cases.

Nomenclature

C_T = propeller thrust coefficient, $T/\frac{1}{2}\rho U^2\pi R^2$
$c_m{}^u$ = Fourier harmonic coefficient of u
J = advance ratio, $U/\Omega R$
m = harmonic number
N = number of propeller blades
R = propeller tip radius
T = propeller thrust
U = axial flight velocity
u,v,w = axial, radial, and tangential induced velocity components, respectively
x,r,θ = cylindrical, propeller-fixed coordinate system
Γ = propeller blade circulation
ρ = fluid density
Ω = propeller angular velocity
$\langle\ \rangle$ = azimuthal mean of induced velocity

Subscripts

p = value at propeller blade
0 = value in propeller plane

Received January 20, 1969. This research was supported by the U. S. Army Research Office–Durham. It was carried out, in part, at Therm Advanced Research Inc., Ithaca, N. Y., under Contract DA-31-124-ARO-D-374 and was completed at Cornell Aeronautical Laboratory Inc. under Contract DAHC04-68-C-0039.

* Research Aeronautical Engineer, Applied Mechanics Department. Member AIAA.

† National Defense Education Act Fellow, Department of Aerospace Engineering. Member AIAA.

I. Introduction

FOR a finite-bladed, lightly loaded propeller in axial cruise flight, the harmonics of the induced velocity components were computed numerically at several field positions in Ref. 1. The propeller was represented by a lifting line and was assumed to have a constant blade-circulation distribution.

This work provided a complement to earlier investigations of the steady part, or zeroth harmonic, of the velocity field.[2-4]

It was shown in Ref. 1 that for a constant circulation distribution the harmonic content of the velocity components could be appreciable as compared to the steady part, especially for a small number of blades and high advance ratios. On the other hand, comparisons[2-4] between the steady parts of the velocity components induced by a constant blade circulation and by an equivalent distribution approximating a Goldstein optimum showed that the velocity fields agree closely outside the slipstream boundary, but are significantly different within the slipstream and immediately upstream of the propeller plane.

The first objective of the present paper, then, is to examine the fluctuating part of the velocity components for the same equivalent blade-circulation distribution that approximates a Goldstein optimum. This will complete the comparisons of the effects of circulation distribution on the velocity field and will distinguish those parts of the flowfield which are, for engineering purposes, independent of the circulation distribution.

The second objective is to investigate similar relationships for a heavily loaded propeller at zero advance ratio, i.e., the static thrust problem. This problem has received considerable attention recently[5-10] because hover is a critical design condition for propeller-driven V/STOL aircraft. These investigations have attempted to eliminate shortcomings in previous analytical approaches to performance prediction. Furthermore, hovering helicopter rotors, which differ from propellers principally in the magnitude of the disk loading, have also been reexamined.[11] For the most part, attention has been focused in these studies on providing propeller (or rotor) designers with improved performance prediction methods. Central to the static thrust problem has been, on one hand, the acquisition of a sound understanding of the significant deformations which the propeller wake must undergo to remain force free and, on the other, the representation of this physical reality with sufficient detail in a theoretically sound mathematical model. Most of the hovering propeller and rotor research has been directed to these ends.[5-13] In addition, the deformation aspects of the wake representation have also been of concern to helicopter rotor forward-flight investigations, some of which have also touched on hover.[14-19]

The present study examines aspects of the flowfield which have had little previous attention in the static case. In parallel with the case of axial cruise, comparisons are made of the velocity induced by equivalent constant and distributed blade circulations, but emphasis has been placed on the velocity components in the propeller plane itself. The characteristics of the flowfield there are examined, including the relationship between the mean inflow over the propeller disk at a given radius, and the instantaneous inflow to the propeller blades at the same radius. Although the induced velocity in the propeller wake was not calculated here, the wake deformations are represented in the mathematical model used for the flowfield calculations.

II. Lightly Loaded Propeller in Cruise

2.1 Mathematical Model

The mathematical model for the propeller is identical to that of Ref. 1. That is, a lightly loaded propeller is considered to be operating in axial cruise flight in a uniform, inviscid, incompressible stream of density ρ and speed U. The propeller has N identical, equally spaced blades of radius R which rotate about their axis at a constant angular velocity Ω. The hub radius is assumed to be zero. A cylindrical, blade-fixed coordinate system (x,r,θ) is chosen such that the propeller disk is normal to the x axis and is located at $x = 0$; $\theta = 0$ locates the position of one of the blades; see Fig. 1.

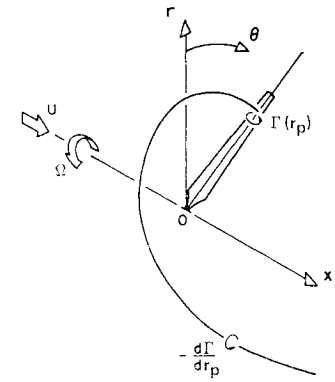

Fig. 1 Coordinate system and nomenclature.

The propeller is represented by the classical lifting-line model of a bound radial vortex line of strength $\Gamma(r_p)$ for each blade, accompanied by a helical vortex sheet of strength $-d\Gamma/dr_p$ trailing from each line, where r_p is the radial distance to any element of the vortex line. The path of each element of the trailing vortex sheet is a helix determined solely by the incoming freestream with translation U and rotation Ω.

The propeller flowfield has been calculated according to the procedures described in Refs. 1 and 2. In brief, the axial, radial, and tangential components of the induced velocity, which are composed of a steady part plus a fluctuating component of period $2\pi/N\Omega$, are expressed in Fourier series form. Thus, for the axial velocity component u, we can write

$$u = U \sum_{m=-\infty}^{\infty} c_m{}^u(x,r)e^{imN\theta} \tag{1}$$

with similar expressions for the radial and tangential components v and w. The Fourier harmonic coefficients $c_m{}^u$ contain contributions from both the bound and trailing vortices and are obtained from the Biot-Savart law. The integral expressions for these coefficients[1-2] are quite complex and must be evaluated numerically.

Since the contribution to the Fourier coefficients from the bound blade vortices involves only a single integration, its calculation is straightforward and is carried out as outlined in Ref. 1. On the other hand, the contribution of the trailing vortex sheets to the Fourier coefficients generally involves double integrals. These integrations are carried out first over the axial extent of the trailing vortex system from the propeller plane to infinity downstream and then over the blade radius. They are computed by a specially programed multiple ten-point double-Gaussian technique. The integrations themselves are straightforward but require a considerable amount of computing time (approximately the square of the time required to do one integration).

The calculations have been carried out for both a uniform circulation,

$$\Gamma(r_p) = \pi JURC_T/N \tag{2}$$

and a nonuniform circulation distribution of the form

$$\Gamma(r_p) = (105\,JURC_T/32N)(r_p/R)(1 - r_p/R)^{1/2} \tag{3}$$

where $J = U/\Omega R$ is the advance ratio and $C_T = T/\frac{1}{2}\rho U^2\pi R^2$ is the ideal thrust coefficient found by neglecting the tangential inflow and the profile drag. The particular form of Eq. (3) was chosen since it approximates the Goldstein optimum fairly well,[2] has the proper square-root behavior near the blade tip, and is simple to use. The constants in Eqs. (2) and (3) are those necessary to express Γ in terms of C_T. For the uniform circulation distribution, the double integration over the trailing vortex system reduces to a single integration since there is only a single vortex of strength Γ trailing from each blade tip together with a line vortex of strength $N\Gamma$ along the x axis.

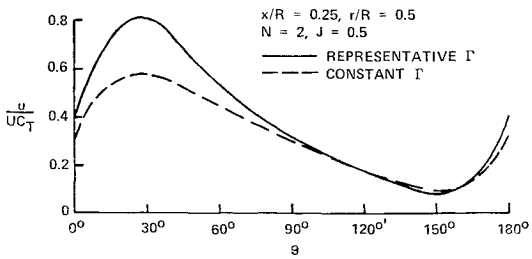

Fig. 2 Effect of circulation distribution on axial induced velocity within slipstream in axial cruise.

2.2 Fluctuating Velocity Field

Calculations of the Fourier coefficients were made at various field points for advance ratios $J = \frac{1}{4}, \frac{1}{2}$, and 1 and for $mN = 2,3,4, \ldots, 9$ in order to compare the results with those previously calculated for the uniform loading.[1] Over-all, both sets of Fourier coefficients exhibited the same behavior. That is, upstream of the propeller, there is a rapid decay with increasing distance from the propeller plane and the coefficients become vanishingly small within about two propeller radii. Downstream of the propeller, the contribution of the bound vortices decays rapidly while that of the trailing vortices takes on a periodic behavior in x with an amplitude which is damped to zero as r increases to infinity.

Once the Fourier coefficients have been found, the calculation of the induced velocity field is easily made by using, say, Eq. (1). Some of the results are shown in Figs. 2 and 3 in which the azimuthal (equivalently, timewise) variation of the axial induced velocity component is plotted for both circulation distributions. In Fig. 2, the velocities are shown for a field point located inside the propeller slipstream. The main feature which is apparent is that, although the magnitudes for each case may differ appreciably, the velocities are approximately in phase with each other. The results for a field location well outside the slipstream are shown in Fig. 3. Again, the velocities are in phase but now their magnitudes at any instant are also very nearly the same. The differences between the magnitudes of the velocities induced by the two circulation distributions are greatest in the vicinity of the trailing vortex sheets, which are at θ values of 28.65° and 57.30° in Figs. 2 and 3, respectively. This is where the influence of the details of the trailing vortex distribution would be expected to be greatest. Of course, as the propeller blade number increases, the magnitude of the fluctuating part of the flow will rapidly decrease, although the steady part will always remain the same. Calculations of the radial velocity component reveal features similar to those of the axial velocity.

All the calculations indicate that a nonuniform circulation distribution has the same effect on the fluctuating part of the flowfield as it does on the steady part. That is, circulation distribution effects are pronounced in the propeller slipstream region and just upstream of the propeller plane but are negligible elsewhere.

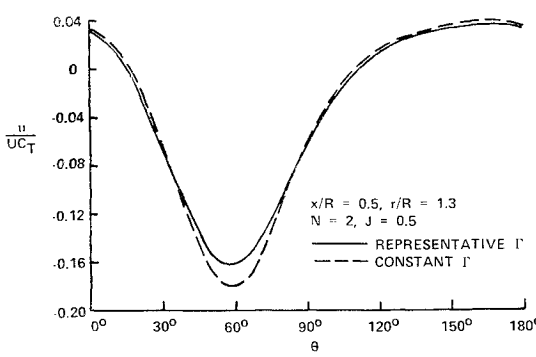

Fig. 3 Effect of circulation distribution on axial induced velocity outside slipstream in axial cruise.

2.3 Asymptotic Behavior of Velocity Field

For field points far from the propeller disk, the limiting behavior of the induced velocity field can be obtained. This is done by approximating the integrands of the Fourier coefficients and carrying out the appropriate simplifications. It is easily shown that the results are independent of the assumed form of the blade circulation for field points outside of the wake; this is to be expected. Two limiting cases are considered: first, letting $r \to \infty$ with x fixed; second, letting $|x| \to \infty$ with r fixed.

In the case of the steady velocities, the integration of the leading term in the Fourier coefficient expansion can be carried out for both limiting cases. The final results are given in Table 1a. From these, it is seen that as $r \to \infty$, the axial component decays faster than does the radial component; for $|x| \to \infty$, the opposite is true. Velocities obtained from these asymptotic formulas agree with the numerically calculated values at distances from the propeller larger than five propeller radii. It should also be noted that the slope of the mean flow streamlines far from the propeller outside the slipstream is given by $\langle v \rangle / \langle u \rangle = r/x$.

For the fluctuating part of the induced velocities, the behavior of the Fourier coefficients has been determined both as $r \to \infty$ and as $|x| \to \infty$. Here, however, the integration of the leading term in the limiting expansion cannot be carried out analytically and so only proportional behavior can be found. The results for this case are given in Table 1b. In contrast to the steady behavior, as $r \to \infty$, the radial harmonic coefficients decay faster than the axial ones while, for $|x| \to \infty$, the axial components decay faster. The limiting behavior of the tangential harmonic coefficients is the same as for the radial ones.

III. Heavily Loaded Propeller in Static Operation

3.1 Mathematical Model

The mathematical model used for propellers in static operation has been developed in Refs. 5–7 and is basically similar to the lightly loaded model discussed above. The principal differences are due to the heavy loading that occurs if the stream speed U is zero. In particular, the elements of the trailing vortex sheets, although of roughly helical shape, have pronounced axial, radial, and tangential deformation. The trajectories of these vortex elements are determined by the condition that they be force free. This condition is satisfied if the local induced velocity along them is such that they are coincident with streamlines of the flow.

Achievement of a truly force-free solution requires an elaborate and lengthy iterative technique involving compu-

Table 1 Asymptotic behavior of induced velocity

a) Steady velocity components

	$\langle u \rangle / UC_T$	$\langle v \rangle / UC_T$
$r \to \infty$	$-xR^2/8r^3$	$-R^2/8r^2$
$\lvert x \rvert \to \infty, r > R$ $x \to -\infty, r \leq R$	$-xR^2/8\lvert x \rvert^3$	$-rR^2/8\lvert x \rvert^3$

b) Fluctuating velocity components

	Axial harmonic coefficient	Radial harmonic coefficient
$r \to \infty$	$1/r^{mN+1}$	$1/r^{mN+2}$
$\lvert x \rvert \to \infty, r > R$ $x \to -\infty, r \leq R$	$1/\lvert x \rvert^{2mN+1}$	$1/\lvert x \rvert^{2mN}$

tation of the induced velocity everywhere on the trailing vortex sheets. Therefore, attention was concentrated on developing a simplified representation of the trailing vortex system that approximates the force-free condition sufficiently well for design purposes. The representation chosen[5-7] is based upon the idea that, since the inflow to the blades must be computed in all cases in order that performance can be predicted on the basis of two-dimensional airfoil data, a relationship that links the velocity along the trailing vortex sheets to the inflow should be sought. Toward this end, it was assumed in Ref. 7 that the envelopes (i.e., r vs x or, equivalently, v/u) describing the contraction of all the trailing vortex elements be fixed according to the exact, heavily loaded, constant circulation, force-free, infinite-blade-number numerical solution of Greenberg and Kaskel.[13] The variations of the axial and tangential velocity components along each trailing element from the inflow values at the blade to the asymptotic values far downstream are based upon previously computed values. These assumptions lead to the radial velocity variations. The axial velocity variations near the propeller tip determine the "effective pitch" of the deformed trailing vortex system and are of principal importance to an adequate theory. In Ref. 7, a double iteration scheme was developed for seeking a reasonably force-free approximation to the flow. It consists of an initial assumption of the axial velocity variations, iteration to determine the inflow, actual computation of the axial variations along the trailing elements and comparison with the assumed variations, revision of the variations as indicated by the comparisons, iteration again to determine the inflow, etc., until convergence of both the inflow and axial velocity variations is achieved.

The results for several cases were not completely satisfactory so far as the double iteration was pursued, particularly in comparisons of computed and experimental performance quantities and computed and assumed contraction patterns. Nevertheless, it is felt that the model contains the essential aspects of the deformation of the trailing vortex wake so that the results given here describe the significant features of the flowfields for these cases, especially in the immediate vicinity of the propeller plane.

3.2 Description of Cases for Static Flowfield Calculations

The calculations presented here were carried out for three propeller loadings that had been investigated principally for inflow and performance.[7] Case I is the three-bladed Curtiss-Wright 3(109652) propeller at a pitch setting of 10° as measured at the seven-tenths radial station. Case II is a three-bladed loading distribution called "Representative Blade Loading 2" in Ref. 7, and case III is a four-bladed loading distribution called "Representative Blade Loading 1."

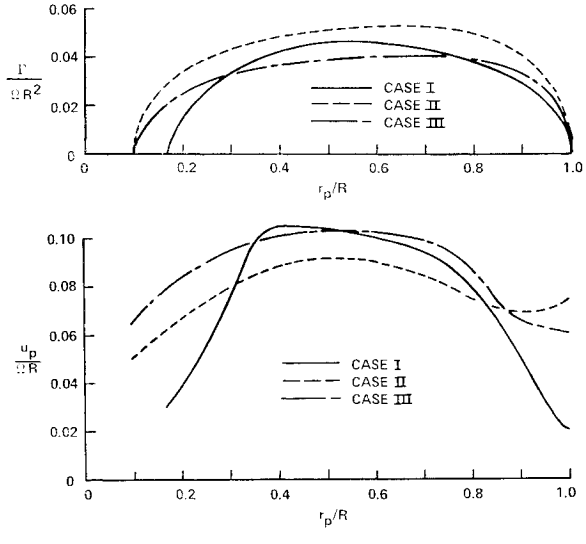

Fig. 4 Characteristics of three propeller loadings in static operation; top) blade circulation distribution; bottom) axial inflow to blades.

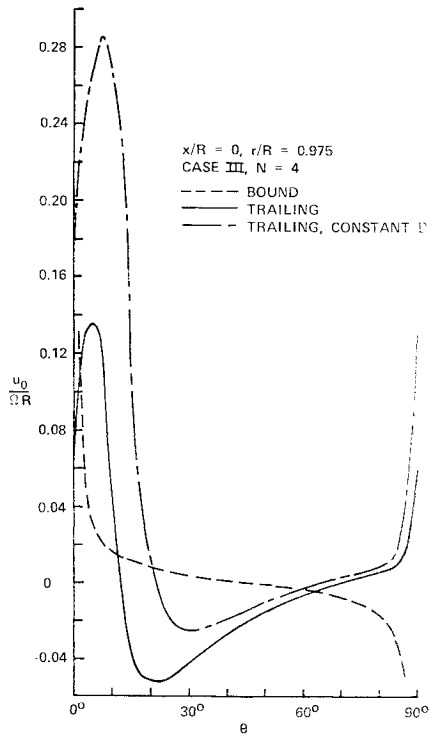

Fig. 5 Effect of circulation distribution on bound and trailing vortex contributions to axial induced velocity within tip radius in propeller plane for static operation.

To illustrate the three cases, the radial distributions of the nondimensional circulation $\Gamma/\Omega R^2$ and axial inflow $u_p/\Omega R$ are reproduced[7] in Fig. 4. It can be seen that, for the three-bladed propeller loadings, u_p is much lower near the tip for case I than for case II so that the effective pitch is lower too. For cases II and III, it is seen that the values of u_p near the tip, and so the effective pitch, are comparable, so that the principal difference between these cases is the number of blades.

The constant circulation equivalents of all three cases were also computed. Equivalence was established by requiring, first, that the constant and distributed circulations have the same ideal thrust at the same Ω and, second, that the single trailing line vortex from each blade tip for constant circulation has the same trajectory as the tip element of the distributed trailing vortex sheet.

The induced velocity field in the static case was computed differently from that of the lightly loaded case. Whereas the azimuthal harmonics of each velocity component were computed for the lightly loaded case, the total of each component was computed here. The computer program used[5-6] is based upon direct integration of the Biot-Savart law over all elements of the bound and trailing vortex systems with appropriate treatment of the continuously deforming trailing vortex sheets. The computations were performed on the IBM 360/65 computing facility at Cornell Aeronautical Laboratory Inc.

3.3 Fluctuating Velocity in Propeller Plane

A series of numerical calculations has been carried out to determine the induced velocity components u_o, v_o, w_o in the propeller plane for cases I–III. The principal results are described here.

The axial component of the induced velocity u_o is made up of a part due to the bound vortex lines representing the

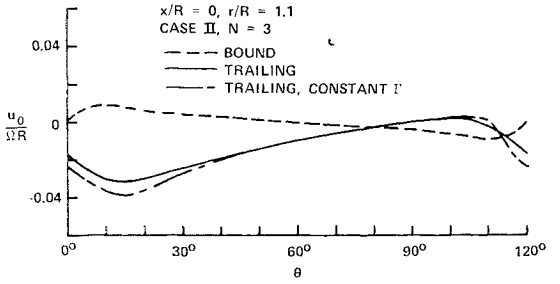

Fig. 6 Effect of circulation distribution on bound and trailing vortex contributions to axial induced velocity outside tip radius in propeller plane for static operation.

blades and a part due to the deformed trailing vortex sheets. An example of these two contributions for case III at the 0.975 radius is presented in Fig. 5 as a function of the azimuthal coordinate θ between two blades of this four-bladed propeller. The bound contribution has exactly the same behavior as for the lightly loaded propeller. It is antisymmetric about the 45° azimuth midway between blades, thus having an azimuthal mean of zero, and it is singular as the lifting line is approached. The trailing contribution has a θ variation which is characteristic in shape of all three cases at this radius. It is positive at the lifting line, increases rapidly to a maximum, then decreases equally rapidly to a negative minimum from which it increases gradually until just before the next blade where the rapid increase to the next maximum begins. In the lifting-line model, the inflow at the blade is induced solely by the trailing vorticity so that the total induced axial velocity is positive at the blades but is largely negative between the blades.

The trailing contribution due to the constant circulation equivalent of case III is also shown in Fig. 5. Although the over-all shape is basically similar, the magnitude is quite different just as it is for light loading. As a result, the mean value $\langle u_o \rangle/\Omega R$ is 0.0396 for constant circulation but -0.0015 for case III.

In contrast to the strong effect of the blade circulation distribution on the magnitude of the induced velocity components for radii within the tip, as demonstrated in Fig. 5, there is only a small effect outside the tip, even as close as at 1.1 propeller radii as shown in Fig. 6 for case II. The trailing contribution to the axial component here is negative for nearly all θ and its mean is negative, whereas the mean axial velocity is identically zero outside the tip in the propeller plane for lightly loaded propellers.[2]

Although comparisons are not presented here, the behavior of the corresponding radial and tangential induced velocity components with regard to the differences between constant and distributed blade circulation is qualitatively the same as for the axial. That is, there are appreciable differences at the 0.975 radius and only small differences at the 1.1 radius.

At the propeller plane, typical changes in the azimuthal variation of the total radial and axial induced velocity components with radial position can be seen in Figs. 7a and 7b, respectively, for case I at radii of 0.7, 0.9, and 0.975. The total radial component shown v_o is due to the contribution from the trailing vortex sheets only, since the bound radial contribution is identically zero in the propeller plane.[2] Most of the axial velocity fluctuation at 0.7 is due to the bound vortices since the fluctuation in the trailing contribution is of comparable magnitude to the fluctuation in the radial component there. As the tip is approached, the magnitude of the fluctuations increases rapidly for both components. Although not shown here, the tangential velocity components, w_o, have fluctuations of comparable percentage magnitude to the others about the mean value of $-N\Gamma(r_p)/4\pi r_p$ that is given by Kelvin's theorem here just as it is for lightly loaded propellers.[2]

A comparison of the influence of effective pitch for three-bladed propellers can be seen in Fig. 8 where the azimuthal variation of the trailing contribution to the axial velocity is given for cases I and II at the 0.975 radius. The shapes are similar and have the same basic nature described above for the four-bladed case III. However, the minimum occurs at a larger θ for case I than for case II because of the geometry of the contraction of the trailing vortex system. Although the contraction of each trailing element is expressed by the same assumed r vs x relationship in both cases, the smaller axial inflow of case I near the tip means that a larger θ is reached for contraction of an element to the same r. In particular, each minimum occurs close to that θ for which the entire trailing vortex system has just contracted enough to be completely within the radius at which the calculations are being made. Here at the 0.975 radius, these θ values are 47.8° for case I and 16.4° for case II.

In all three cases, the axial induced velocity from the trailing vortex system varies extremely rapidly with θ in the immediate vicinity of the blades, especially at radii near the tip. Although this variation is in the propeller plane, previous computations[7] show a rapid change along the elements of the trailing vortex sheets as well. These rapid variations

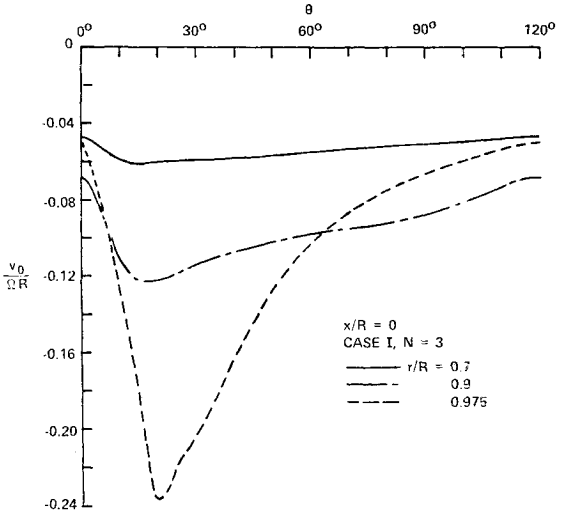

a) Radial induced velocity

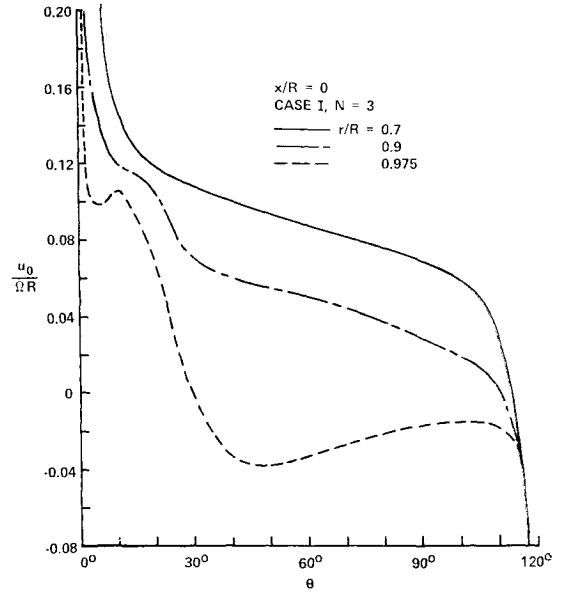

b) Axial induced velocity

Fig. 7 Influence of radius on induced velocity fluctuations in propeller plane for static operation.

over distances as small as a chord length cast considerable doubt on the applicability of the lifting-line model because they imply a significant induced camber effect.

The results presented can be used to assist in the interpretation of flow visualization experiments which have been made. For example, smoke pictures such as those presented in Ref. 9 seem to indicate that the flow enters the propeller plane from behind the blade near the tip. Although cases may exist for which the instantaneous axial velocity near the tip is negative at the blades as well as between them, all cases considered here have positive axial velocity at the blades despite a large region of negative axial velocity between them.

3.4 Mean and Instantaneous Inflow

The relationship between the mean inflow at a given radius in the propeller plane and the instantaneous inflow to the blade at the same radius is important in interpreting and applying mean flow results from infinite-blade-number theories.

The ratios of the mean to instantaneous axial $\langle u_o \rangle / u_p$ and radial $\langle v_o \rangle / v_p$ inflow are given as a function of radius in Figs. 9a and 9b, respectively, for cases I–III. Computations were made outboard of the 0.7 radius since there appeared to be little difference between the mean and instantaneous inflow at inboard radii. Although these ratios differ considerably in magnitude from the lightly loaded results for constant circulation[1] and for Goldstein optimum circulation distributions,[20] qualitatively, they display similar relationships. That is, a comparison of the three-bladed cases indicates that, at a given radius near the tip, the mean inflow is closer to the instantaneous values for case I than for case II because the former has a lower effective pitch. Further, a comparison of the cases with comparable effective pitch shows that the mean inflow is closer to the instantaneous for case III than for case II because the former has a larger number of blades. The mean and instantaneous tangential inflow compare with one another qualitatively like the case I axial inflow. Therefore, the magnitudes of the axial and tangential ratios differ. This is in contrast to lightly loaded propellers for which the axial and tangential ratios are identical; i.e., $\langle u_0 \rangle / u_p = \langle w_0 \rangle / w_p$ in all cases.[1]

In view of the observations that the mean radial inflow is greater than the instantaneous, whereas the mean axial inflow is less than the instantaneous (and may even be negative), the streamline patterns (i.e., $\langle v \rangle / \langle u \rangle$) computed by infinite-blade-number models may be somewhat misleading.

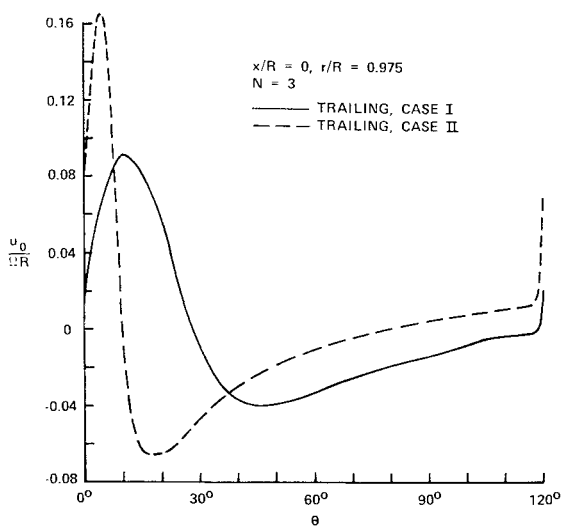

Fig. 8 Influence of effective advance ratio on trailing vortex contribution to axial induced velocity in propeller plane for static operation.

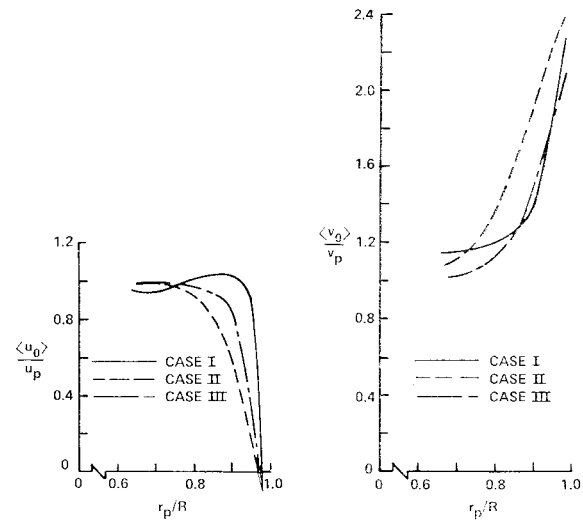

a) Axial inflow **b) Radial inflow**

Fig. 9 Ratios of mean inflow in propeller plane to instantaneous inflow at propeller blades for three cases in static operation.

For example, the strong initial contraction predicted by Greenberg and Kaskel[13] may not be representative of the instantaneous values along the elements of the trailing vortex sheets as was assumed in Ref. 7.

IV. Conclusions

Numerical computations of the fluctuating flowfield of a lightly loaded propeller in axial cruise with both a constant blade circulation distribution and one approximating a Goldstein optimum indicate that, within the slipstream and just upstream of the propeller, the induced velocities are highly dependent upon the circulation shape. On the other hand, in the remainder of the field, the induced velocities can be considered independent of the circulation shape for practical purposes, provided the total loading is the same. Asymptotic formulas derived for the far-field induced velocities agree with numerically computed values at distances greater than five blade radii from the propeller. For heavily loaded propellers in static operation, limited calculations for three cases yield similar results for the velocity components induced by constant and distributed blade circulations.

For a propeller in static operation, the basic shape of the azimuthal variation of the velocity components in the propeller plane does not depend significantly on the number of blades or the effective pitch of the deformed trailing vortex sheets. Differences in the detailed shape of the azimuthal variations of the velocity components arise in large measure from the rate of contraction of the elements of the trailing vortex sheets with respect to azimuth. The fluctuations induced by the trailing vortex system become much more pronounced as the tip is approached, i.e., outboard of the 0.9 radius of the propeller. For all cases investigated, the axial velocity component at the 0.975 radius is positive at the blades, but is sufficiently negative at azimuthal positions between blades that the mean is negative. The ratios of the mean to the instantaneous inflow components as a function of radius differ qualitatively with blade number and effective pitch in the same manner as for light loading, although the magnitudes of the ratios are quite different.

The rapid variation of the axial induced velocity over distances as small as a blade chord length implies an induced camber effect which casts doubt on the applicability of the lifting-line model for accurate prediction of the static performance. Nevertheless, the flowfield characteristics re-

vealed in the calculations aid the interpretation of both flow visualization results and theoretical results for infinite-blade-number models.

References

[1] Hough, G. R., "A Numerical Study of the Fluctuating Flowfield of a Uniformly Loaded Propeller," *Journal of Aircraft*, Vol. 4, No. 1, Jan.-Feb. 1967, pp. 36–41.

[2] Hough, G. R. and Ordway, D. E., "The Generalized Actuator Disk," *Developments in Theoretical and Applied Mechanics*, Vol. 2, Pergamon, Oxford, 1965, pp. 317–336.

[3] Hough, G. R. and Ordway, D. E., "The Steady Velocity Field of a Propeller with Constant Circulation Distribution," *Journal of the American Helicopter Society*, Vol. 10, No. 2, April 1965, pp. 27–28.

[4] Hough, G. R. and Ordway, D. E., "Mean Flow Streamlines of a Finite-Bladed Propeller," *Journal of Aircraft*, Vol. 4, No. 6, Nov.-Dec. 1967, pp. 561–562.

[5] Erickson, Jr., J. C. et al., "A Theory for VTOL Propeller Operation in a Static Condition," TR 65-69, Oct. 1965, U. S. Army Aviation Materiel Labs., Fort Eustis, Va.

[6] Erickson, Jr., J. C. and Ordway, D. E., "A Theory for Static Propeller Performance," *Proceedings, CAL/USAAVLABS Symposium on Aerodynamic Problems Associated with V/STOL Aircraft*, Vol. 1, Technical Session 1, Cornell Aeronautical Lab. Inc., Buffalo, N. Y., June 1966.

[7] Erickson, Jr., J. C., "Theoretical and Experimental Investigations of V/STOL Propeller Operation in a Static Condition," TR 69-55, U. S. Army Aviation Materiel Labs., Fort Eustis, Va., to be published.

[8] Trenka, A. R, "Prediction of the Performance and Stress Characteristics of VTOL Propellers," *Proceedings, CAL/USAAVLABS Symposium on Aerodynamic Problems Associated with V/STOL Aircraft*, Vol. 1, Technical Session 1, Cornell Aeronautical Lab. Inc , Buffalo, N. Y., June 1966.

[9] Adams, G. N., "Propeller Research at Canadair Limited," *Proceedings, CAL/USAAVLABS Symposium on Aerodynamic Problems Associated with V/STOL Aircraft*, Vol. 1, Technical Session 1, Cornell Aeronautical Lab. Inc , Buffalo, N. Y., June 1966.

[10] Gartshore, I. S., "An Application of Vortex Theory to Propellers Operating at Zero Advance Ratio," TN 66-3, June 1966, Mechanical Engineering Research Labs., McGill Univ., Montreal.

[11] Jenney, D. S., Olson, J. R., and Landgrebe, A. J., "A Reassessment of Rotor Hovering Performance Prediction Methods," *Journal of the American Helicopter Society*, Vol. 13, No. 2, April 1968, pp. 1–26.

[12] Gray, R. B., "An Aerodynamic Analysis of a Single-Bladed Rotor in Hovering and Low Speed Forward Flight as Determined from Smoke Studies of the Vorticity Distribution in the Wake," R. 356, Sept. 1956, Aeronautical Engineering Dept., Princeton Univ., Princeton, N. J.

[13] Greenberg, M. D. and Kaskel, A. L., "Inviscid Flow Field Induced by a Rotor in Ground Effect," CR-1027, May 1968, NASA.

[14] Tararine, S., "Experimental and Theoretical Study of Local Induced Velocities over a Rotor Disc," *Proceedings, CAL/TRECOM Symposium on Dynamic Load Problems Associated with Helicopters and V/STOL Aircraft*, Vol. 1, Cornell Aeronautical Lab. Inc., Buffalo, N. Y., June 1963

[15] Piziali, R. A., "Method for the Solution of the Aeroelastic Response Problem for Rotating Wings," *Journal of Sound and Vibration*, Vol. 4, No. 3, 1966, pp. 445–489.

[16] Crimi, P., "Prediction of Rotor Wake Flows," *Proceedings, CAL/USAAVLABS Symposium on Aerodynamic Problems Associated with V/STOL Aircraft*, Vol. 1, Technical Session 2, Cornell Aeronautical Lab. Inc., Buffalo, N. Y., June 1966.

[17] DuWaldt, F. A., "Wakes of Lifting Propellers (Rotors) in Ground Effect," Rept. BB-1665-S-3, Nov. 1966, Cornell Aeronautical Lab. Inc., Buffalo, N. Y.

[18] Scully, M. P., "A Method of Computing Helicopter Vortex Wake Distortion," TR 138-1, April 1967, Aeroelastic and Structures Lab., MIT, Cambridge, Mass.

[19] Lehman, A. F., "Model Studies of Helicopter Rotor Flow Patterns in a Water Tunnel," Paper 207, Proceedings, American Helicopter Society 24th Annual Forum, Washington, D. C., May 1968.

[20] Tibery, C. L. and Wrench, Jr., J. W., "Tables of the Goldstein Factor," Rept. 1534, Dec. 1964, David Taylor Model Basin, Washington, D. C.